Reversible *versus* Irreversible Binding of Transferrin to Polystyrene Nanoparticles: Soft and Hard Corona

Silvia Milani,[†] Francesca Baldelli Bombelli,[‡,§,⊥] Andrzej S. Pitek,[‡,§] Kenneth A. Dawson,[‡,§,*] and Joachim Rädler[†,*]

[†]Faculty of Physics, Ludwig-Maximilians-Universität, Geschwister-Scholl-Platz 1, 80539 Munich, Germany, [‡]Centre for BioNano Interactions, School of Chemistry and Chemical Biology, and [§]Conway Institute for Biomolecular and Biomedical Research, University College Dublin, Belfield, Dublin 4, Ireland, and [⊥]School of Pharmacy, University of East Anglia, Norwich, NR4 7TJ, United Kingdom

ABSTRACT

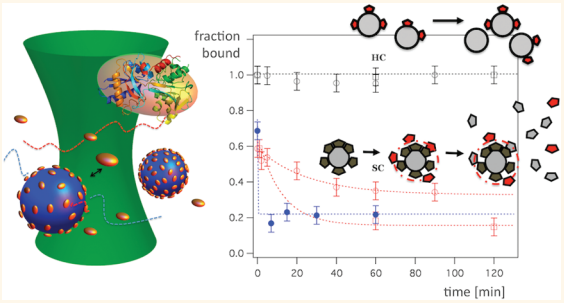

Protein adsorption to nanoparticles (NPs) is a key prerequisite to understand NP—cell interactions. While the layer thickness of the protein corona has been well characterized in many cases, the absolute number of bound proteins and their exchange dynamics in body fluids is difficult to assess. Here we measure the number of molecules adsorbed to sulfonate ($PSOSO_3H$) and carboxyl-(PSCOOH) polystyrene NPs using fluorescence correlation spectroscopy. We find that the fraction of molecules bound to NPs falls onto a single, universal adsorption curve, if plotted as a function of molar protein-to-NP ratio. The adsorption curve shows the build-up of a strongly bound monolayer up to the point of monolayer saturation (at a geometrically defined protein-to-NP ratio), beyond which a secondary, weakly bound layer is formed. While the first layer is irreversibly bound (hard corona), the secondary layer (soft corona) exhibits dynamic exchange, if competing unlabeled is added. In the presence of plasma proteins, the hard corona is stable, while the soft corona is almost completely removed. The existence of two distinct time scales in the protein off-kinetics, for both NP types studied here, indicates the possibility of an exposure memory effect in the NP corona.

KEYWORDS: fluorescence correlation spectroscopy (FCS) · nanoparticles—proteins interaction · protein corona · bionano interface · Transferrin

Nanoparticles receive growing attention in every sector of science and technology; their size, structure, and chemical properties open up a vast range of technical applications and novel approaches in basic research. However, it is clear that, both to ensure ourselves of their safety in general and to apply them as therapeutic tools, it will be necessary to understand from a more fundamental point of view how nanoparticles interact with living organisms. In this context, it has been pointed out that in a biological environment it is not the nanoparticle as such, but rather its surface composition that governs interaction with living matter. Upon encountering biological fluids the surface layer of nanoparticles, depending on size and composition, is covered by biomolecules (including proteins) and possibly extracellular matrix components forming what is described as a "corona". This corona is likely to play the dominant role in determining how nanoparticles distribute within the body and eventually the particle fate.[1−6] The protein corona is what interfaces with the cell. Thus, corona composition can involve not just competitive binding with immunoglobulins or other opsonins (promoting receptor-mediated phagocytosis), but also a variety of signaling molecules, inducing a variety of biological effects.[7] As a result, protein−NP adsorption has been studied widely and may be linked to biodistribution and nanotoxicity mechanisms.[8−10]

Various techniques such as ITC,[11−13] surface plasmon resonance,[14] QCM,[15] and DCS[16] have been employed to shed light on the affinities of proteins for nanoparticles.[17−23] Recently also fluorescence correlation spectroscopy (FCS) has been used to determine the binding constant of protein to NPs from the shift in the diffusion time of the NPs.[24−28]

In many of these works Langmuir absorption isotherms are employed to measure the equilibrium binding constants of the adsorption process. However, there is increasing evidence that the adsorption of proteins is not reversible on microscopic time-scales[18,21] suggesting that the use of equilibrium concepts, such as adsorption

* Address correspondence to joachim.raedler@physik.uni-muenchen.de, Kenneth.A.Dawson@cbni.ucd.ie.

Received for review December 19, 2011 and accepted February 22, 2012.

Published online February 22, 2012
10.1021/nn204951s

isotherms, may not be valid.[16] Yet, reversibility is an issue that is of paramount importance with regard to how we think about protein–NP interactions in a biological environment.[29–31] Reversibility implies that adsorbed protein comes off once the bulk concentration of protein is lowered and second that the same composition of adsorption layer is found independent of the path of preparation or order by which components were added to the solution. It is generally accepted that abundant plasma proteins bind to nanoparticles (sometimes referred to as opsonization). However, over time, some of these proteins may be displaced by other proteins with higher affinity, some of them being much less abundant, and having significant biological roles.[32,33] A related process occurs on flat surfaces (the Vroman effect[34]), but as yet no detailed understanding of the nature of this process for nanoparticles exists. In the model system, the subject of this study, the radii of curvature of particles we explore are quite large compared to the proteins (unlike biological fluids where much larger assemblies can be involved). Still, there are differences, even for this simplified model; the preparation of nanoparticles involves surface terminations chemistries far different from that of bulk substance, and the particle diffusion modifies the diffusional access from more distant proteins over extended times. Therefore we cannot yet be definitive about the detailed nature of the processes by which the first layer is first formed. Still, in practical terms the surface layer of nanoparticles has been hypothesized to consist of a hard shell of proteins (the hard corona (HC) assumed irreversibly bound) and a secondary layer of macromolecules (named the soft corona (SC)) that is thought to reversibly interchange with other molecules in solution that compete for binding to the NP surface.[1,8,35,21] Limited clear evidence for the presence of this two-time-scale conception has hitherto been presented, but it has hard practical significance. Thus, we consider that, for a given biological event, there is a characteristic time-scale that governs it (for example particle internalization events may occur on a time-scale of several minutes), and that biomolecules that reside longer on the nanoparticle surface than this time may contribute to biological identity of the nanoparticle.[36] Given the slow exchange of proteins from the hard corona, this layer of proteins may be considered irreversibly bound,[16] and thereby biologically relevant, whereas if the soft corona exchanges quickly enough, it may be neglected. Still, in principle, this must still be established based on explicit understanding of the exchange times also of the soft corona, about which little is known. The present paper establishes the nature of these two processes, as well as a methodology for future studies.

It has also been reported that NPs reaching the vascular system, *via* the lungs, access the brain more effectively than those delivered directly into the bloodstream.[6,37,38] This also raises the question of the degree to which even the relatively immobile hard corona is exchanged, depending on different exposure routes. The lack of information on the dynamics of protein exchange is mainly due to a shortage of techniques that allow for assessment of the binding and unbinding of specific proteins to nanoparticles in the presence of human body fluids. Fluorescence correlation spectroscopy (FCS) is a unique technique in that it can measure the concentration and diffusion time of fluorescently labeled particles or proteins in solution. The technique allows quantitative measurements of adsorption in agreement with independent techniques and theoretical adsorption models as, for example, shown for cationic peptides binding to negatively charged vesicles.[39] Since FCS detects the fluorescently labeled component only, the technique allows reliable measurements also in turbid media like blood plasma, making it potentially useful for analyses of practical biological interest.[40,41]

Here, we measure adsorption of the protein Transferrin to sulfonate polystyrene nanoparticles ($PSOSO_3H$) and carboxyl–polystyrene (PSCOOH) nanoparticles, as a model system. Transferrin (Tf) is one of the most abundant blood glycoproteins and responsible for the transport of iron (Fe(III)) in the circulatory system. In particular Tf has been used as a targeting agent to overcome the lack of specificity of conventional therapeutic nanoparticles or contrast media.[42] Using FCS we measured the adsorption of Transferrin molecules to NPs by numbers. We show that adsorption depends on the molar protein-to-NP ratio and that there exists a defined ratio where a full monolayer of protein is reached. It is striking that the FCS analysis allows us to discriminate a secondary layer beyond this critical ratio, which is distinct from the first monolayer of adsorption, allowing us to obtain information on the soft corona for the first time. The first monolayer (hard corona) is irreversibly bound, while the secondary layer (soft corona) is capable of exchanging protein with the solution. In particular we show that the outer layer of adsorbed Transferrin is removed by the presence of plasma by competitive binding of blood plasma proteins.

RESULTS AND DISCUSSION

The Fraction Bound. Figure 1a shows a schematic drawing of Transferrin molecules and NPs diffusing in a solution illuminated by a focused laser beam. Here Transferrin (the adsorbant) is fluorescently labeled, while the NPs (the substrate) remain unlabeled. Binding is detected by a change in the diffusion constant of the labeled Transferrin, and the fraction of bound Transferrin molecules is determined by a two-component fit to the time autocorrelation function of the FCS signal.[39,40] When unlabeled NPs are added to a

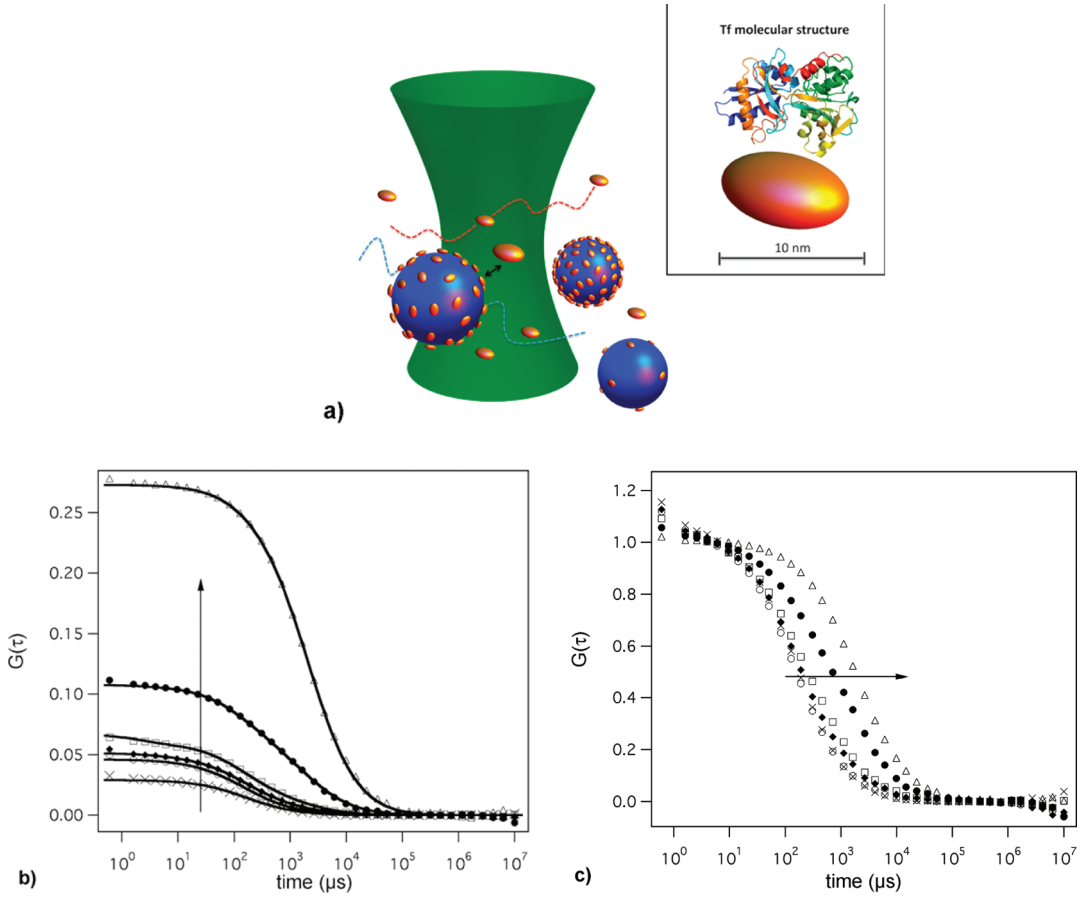

Figure 1. (a) Schematic drawing of Transferrin molecules and coated NPs diffusing within the fluorescent correlation spectroscopy apparatus. (b) Autocorrelation functions of Tf-488 binding to $PSOSO_3H$ NPs in PBS. Autocorrelation curves are shown for 0, 0.5, 1, 2, 5, and 40 μg/mL NPs concentrations, corresponding to 0% (cross), 5% (circle), 14% (full diamond), 22% (square), 56% (full circle), and 99% (triangle) fraction bound. The lines through the data represent the best fit with a two-component fit model. (c) Normalized autocorrelation curves exhibit a systematic shift toward longer correlation times indicating an increasing fraction of bound protein with an increase in the NPs concentration.

solution of labeled Transferrin the amplitude of the time auto correlation $G(0)$ increases (Figure 1b). At the same time the diffusion time shifts to larger values as best seen in the normalized plot of the $G(t)$ (see Figure 1c). A two-component fit to $G(t)$ allows us to quantify the amplitude of the slow (bound) and fast (free) component in the data and to determine the fraction of bound Transferrin. To improve the robustness of the fitting the diffusion time of Tf in the absence of NPs and the size of coated NPs, when all the protein is adsorbed on the NPs surface, are kept as fixed parameters. The hydrodynamic radius of Tf as determined by the FCS diffusion time, is 3.6 nm in good agreement with the value obtained for unlabeled Tf (R_h = 3.72 nm) by DLS.[43] Likewise, the hydrodynamic radius of NPs fully covered with Transferrin turns out to be 51 nm in good agreement with R_h = 48.6 nm of Transferrin coated NPs measured by DLS (see also Table 1 in the Supporting Information). Details of the two-component analysis have originally been described by Rusu *et al.*[39] and can be found in the Experimental section.

We measured the fraction of bound Tf as a function of NPs added (see Figure 2a). As expected the fraction of bound protein increases with increasing NPs concentration. Yet the adsorption behavior depends on the amount of protein present in solution. It is worth noting, however, that Langmuir adsorption isotherms apparently fit the experimental data quite well. Likewise, we measured the fraction of Tf bound to NPs as a function of the amount of Tf added. Here, the adsorption of protein depends on the number of available NPs and, accordingly, the apparent binding constants would be dependent on the NPs concentration (see Figure 2b).

In contrast, in a normalized representation of fraction-bound *versus* the concentration ratio of protein to NPs the data fall onto a universal curve (see Figure 3a). The fraction-bound ratio is equal to 1 up to the critical value where the number of Tf per NPs reaches its maximum value. After this point, which we called the saturation point, the fraction bound decreases. This behavior is captured by the simple picture that, as long as the NP surface is not fully covered, any free Tf molecules will bind strongly to NPs. Beyond the point of saturation Tf continues binding to NP, though to a lesser extent. Note that this behavior is not dependent

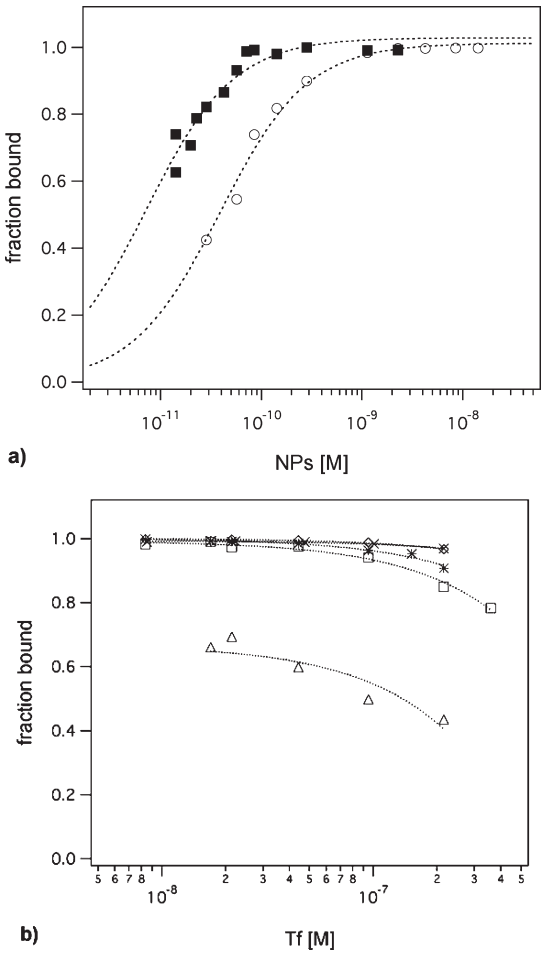

Figure 2. FCS measurements of Tf binding to $PSOSO_3H$ in PBS. The fraction bound was deducted from FCS data similar to those shown in Figure 1. (a) Experiments performed at a fixed concentration of Tf (full square, 2.5 μg/mL; circles, 20 μg/mL) by adding NPs. Dashed lines are Langmuir adsorption curves. (b) Experiments performed at a fixed concentration of NPs (triangle, 1 μg/mL; square, 10 μg/mL; asterisk, 25 μg/mL; diamond, 50 μg/mL; and cross, 100 μg/mL) by adding Tf. Dotted lines represent linear fit to the data to guide the eyes.

on the sample preparation. From the onset of fraction-bound decrease, we retrieve the molar ratio $x^*_c \approx 300 \pm 100$ for the saturation point. Thus, given a NP surface of roughly 20000 nm^2 for a nanoparticle of 82 nm in size (see DLS measurements in the Supporting Information), it is inferred that a single Tf occupies a surface area on the NPs of about 66 nm^2. This value is slightly larger than the Transferrin surface area (42 nm^2),[25] as estimated from the known molecular structure of Transferrin.[44]

Strong Binding Model. The finding of an universal adsorption behavior as a function of molar protein/NP ratio is to first-order well described by an adsorption model that assumes a strong interaction of protein with uncovered NP surface and a negligible interaction of protein with a NP surface saturated with a protein monolayer. According to this "strong binding model", proteins bind to a NP until all free space on the NP surface is fully covered.

Introducing the unitless molar ratio x = [Tf]/[NPs] the fraction of bound protein to total protein is given by

$$f = \frac{[Tf]_{bound}}{[Tf]_{total}} = \begin{cases} 1 & \text{if } x \le x_c^* \\ x_c^*/x & \text{if } x > x_c^* \end{cases} \quad (1)$$

where x_c^* represents the critical molar ratio of a saturated monolayer coverage. In a log−log plot (Figure 3a) the model and data are shown. The gray line represents the model, which assumes no interaction between proteins and NPs after the critical ratio. Remarkably, all data points fall onto a universal curve, which qualitatively shows the predicted behavior, that is, full adsorption up to x_c^* and a decreasing fraction bound beyond. However the fraction bound does not decrease as rapidly as predicted by the simple strong binding model indicating that more protein is bound. The latter fact can be explained, if we allow a secondary layer to form by weak protein−protein interaction. In fact we can use the strong binding model to quantify the amount of Tf, bound in the secondary layer, by calculating the difference between the experimental data and the hypothetical first layer (gray line).

In Figure 3b the surface coverage, Γ eq 2, in units number of molecules per NP, is plotted against the molar ratio protein/NPs. The figure represents values calculated from the measured fraction bound and the known total number of proteins per NP.

$$\Gamma = \begin{cases} [Tf]/[NPs] & \text{if } x \le x_c^* \\ [Tf](f - f_{\text{strong binding model}})/[NPs] & \text{if } x > x_c^* \end{cases} \quad (2)$$

where f is the measured fraction bound and $f_{\text{strong binding model}}$ is obtained by eq 1.

The dashed lines indicate the number of proteins at the saturation point, that is, when the first layer is completed, as well as the estimated level of the second and third layer. The later number can be inferred by geometrical consideration knowing the hydrodynamic radii of the pristine nanoparticles and coated nanoparticles. The number of molecules adsorbed on the second layer has to be 300 times the ratio of the areas of coated and pristine nanoparticles. Because this value does not reach the number of proteins measured by our model, another, third layer of molecules (white corona in Figure 3c) has to be adsorbed. In Figure 3b the red line indicates a BET isotherm to describe the adsorption of the second and third layer (see Supporting Information for details).

Although the number of molecules and the existence of a secondary and ternary layer inferred by the FCS measurements may appear very high, it is worthwhile to note that the same order of magnitude for the corona was estimated previously for a related system from the increase of the effective hydrodynamic radius.[26,45] There remains, however, the caveat that adsorption might be more heterogeneous than assumed in the model. AFM imaging has recently

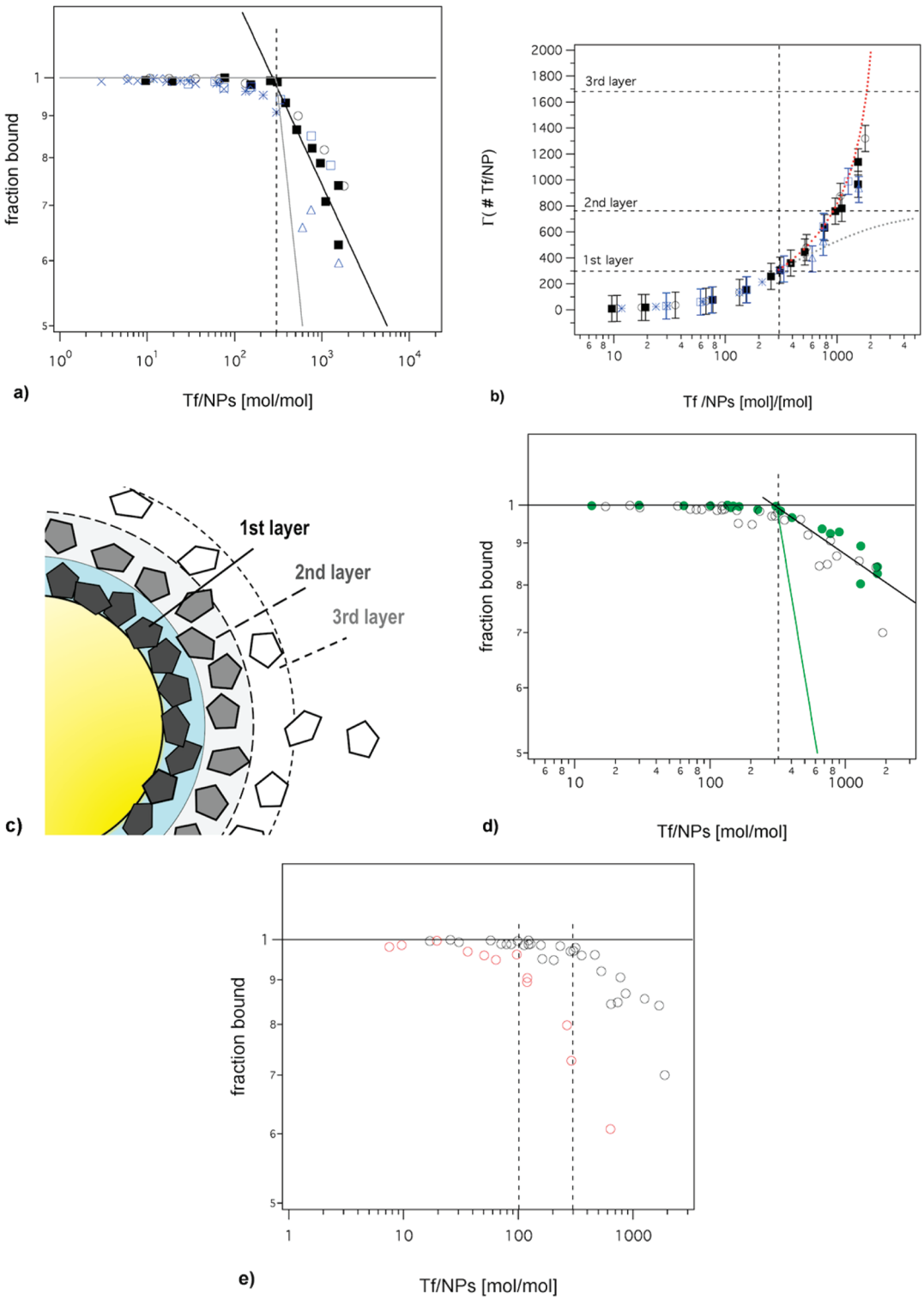

Figure 3. (a) A normalized representation (fraction bound *vs* the ratio of protein to NPs) of the same data as presented in Figure 2a,b shows a universal behavior. The vertical dashed line indicates the ratio of full surface coverage. The gray line represents the theory of a single strongly bound monolayer as discussed in the text: titration of NPs to Tf (black symbols) or titration of Tf to NPs (blue symbols). (b) Surface coverage, Γ, in number of Tf molecules bound per NP. The number of Tf bound beyond full coverage was inferred by subtracting the hypothetical first monolayer of molecules (gray line) from experimental data. In the graph the dashed gray line represents a hypothetical Langmuir adsorption where the maximum number of sites available was determined by knowing the size of coated NPs. The red line represents a hypothetical BET adsorption. (c) Schematic drawing of a nanoparticle covered by layers of Tf as shown in panel b. (d) Normalized representation (fraction bound *vs* the ratio of protein to NPs) of Tf bound to PSCOOH and $PSOSO_3H$ 100 nm in MES buffer: PSCOOH, black circles; $PSOSO_3H$, green circles. (e) Normalized representation (fraction bound *vs* the ratio of protein to NPs) of Tf bound to PSCOOH 71 nm, black circles, and PSCOOH 41 nm in MES buffer, red circles. Dashed lines represents an estimation of the number of molecules adsorbed on both NPs, which scales by the factor expected from geometrical increase in surface area per NP.

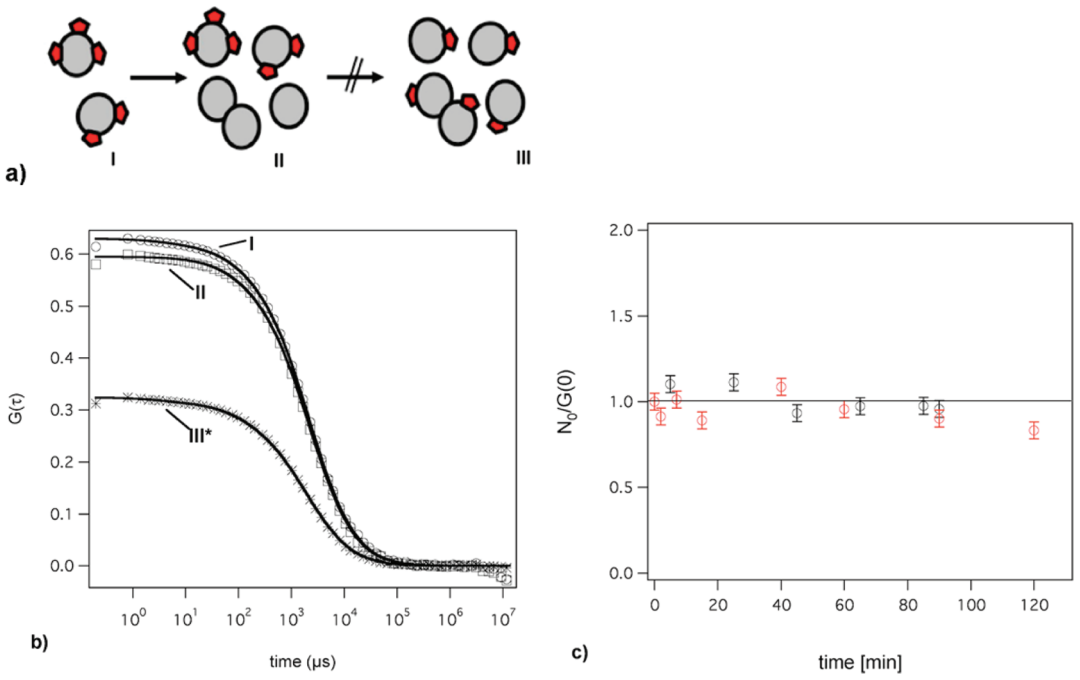

Figure 4. (a) Schematic drawing of the reversibility experiment. NPs are added to half-coated NPs. In case proteins exchange and redistribute, the apparent number of fluorescent NPs should increase. (b) Autocorrelation functions and fits (black line) of 7 μg/mL Tf-488 binding to 25 μg/mL $PSOSO_3H$ NPs (black circles, 50% coated NPs) and to 275 μg/mL $PSOSO_3H$ NPs (black asterisk, 5% coated NPs) in PBS. Black square represents the autocorrelation function of half-coated NPs after 10 times more concentrate pristine NPs have been added. (c) Time course of the number of NPs (per focal volume) normalized by the value N_0 collected before the protein addition. No decrease of the N_0/N is observed for $PSOSO_3H$ NPs (black circles) after 90 min. Also the trend of N_0/N for PSCOOH NPs (red circles) remains almost constant around 1.

revealed the formation of patches of isolated multilayers on a polystyrene surface covered with BSA.[46]

The qualitative features of the strong binding model should be independent of the surface chemistry and size of the particles. Hence for comparison, Figure 3d shows the fraction of Transferrin bound to carboxylate nanoparticles in MES buffer as compared to the $PSOSO_3H$ NPs discussed above. The adsorption curve as a function of molar Tf/NPs ratio shows a similar plateau followed by a decrease of the fraction bound with increasing Tf/NPs ratio. However, it appears that the adsorption of Transferrin to polystyrene NPs with carboxylic acid groups does not show a clearly distinct saturation point. Although there is a regime of 100% fraction bound, proteins are exchanged with the bulk solution at submonolayer concentration regime. While the pH of the solution does not affect too much the point of monolayer saturation for $PSOSO_3H$ NPs, it is worth noting that no interaction between Tf and PSCOOH nanoparticles has been detected in PBS.[19] The protein adsorption on PSCOOH nanoparticles of 71 and 41 nm in MES buffer is also compared. Figure 3e shows that the NP size alters the critical protein/NP ratio of saturation by the factor expected from the geometrical increase in surface area per NP. As we said above, nanoparticles bearing carboxylic acid groups do not show a neat kink between strongly and weakly bound proteins that would allow measurement of the number of molecules adsorbed in the first layer. However, an approximated estimation of 300 molecules might be taken as a number of proteins adsorbed on 71 nm PSCOOH nanoparticles (see dashed line in Figure 3e). Since the smallest NPs are 41 nm in size as measured by DLS (see also Supporting Information), there should be enough room to accommodate a maximum of 100 molecules. Remarkably, this value coincides within the experimental error, with that in which the fraction bound to the smallest NPs starts decreasing.

Reversibility. We use FCS to quantify the exchange of proteins from the hard and soft corona. We hypothesize that the first monolayer of proteins reduces the high bare surface free energy of the nanoparticle by binding irreversibly to it. Despite the fact that the surface free energy has been lowered, the bound layer has a different average structure to the dissolved free Transferrin, and thereby forms a new interface with it, this time on more typical thermal energy scales, restoring meaningful exchange, and equilibrium considerations. To verify this hypothesis we employed FCS. The FCS autocorrelation function yields the concentration of fluorescent particles per focal volume. To determine the off-rate of Tf from the hard corona we study Tf-NPs at a protein−NP ratio corresponding to one-half of the saturation value, that is, where NPs are loaded on average with half the capacity of the first monolayer (see state I in the schematic Figure 4a). We then add 10× more uncoated NPs and follow the total

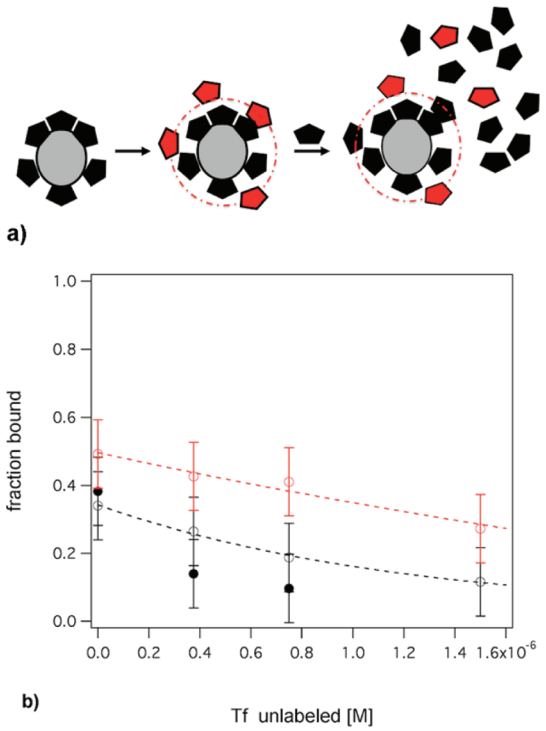

Figure 5. (a) Schematic drawing of competitive unbinding. First a monolayer of unlabeled Tf is adsorbed, second a labeled Tf is added. Finally unlabeld Tf is added and exchanged with the labeled Tf-488 of the secondary layer. (b) FCS detects the decrease of the fraction of bound Tf-488 (black full and empty circles, $PSOSO_3H$ in PBS; red circles, PSCOOH in MES). Dashed line represents a single exponential fit to the data.

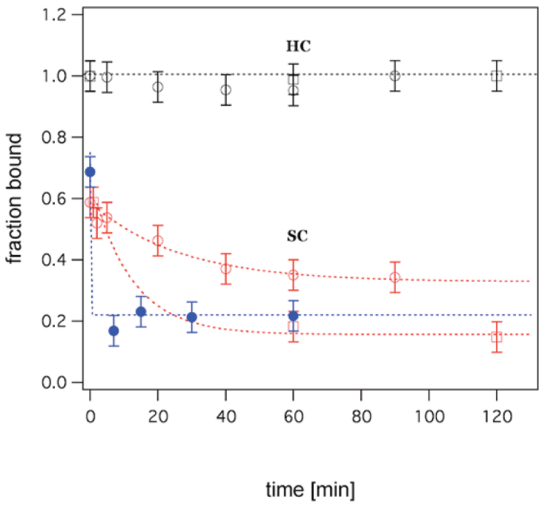

Figure 6. Competitive unbinding in the presence of blood plasma proteins. There is no unbinding of Tf-488, if NPs are with a monolayer (hard corona, HC) only (black circles, 5% plasma; black square, 10% plasma). In case of a labeled secondary layer (as seen in figure 5), the addition of plasma (red and blue circles, 5% plasma added to $PSOSO_3H$ and PSCOOH NPs, respectively; red square, 10% plasma added to $PSOSO_3H$) removes the secondary layer (soft corona, SC). Red dashed lines are obtained by a single exponential fit, yielding the off-times $\tau_{5\%}$ = 26 min and $\tau_{10\%}$ = 12 min. Even the secondary layers of PSCOOH NPs are removed by the addition of 5% plasma.

number of fluorescent objects by FCS (state II in Figure 4a). If proteins are exchanged between NPs, the number of fluorescent NPs should increase (state III in Figure 4a). Figure 4b shows the time autocorrelation function of states I and II. The experiment shows that the amplitude of the time-correlation does not evolve. As shown in Figure 4c after 90 min of being monitored, the normalized number of NPs remains constant with time. As a control we mix the equivalent amount of NPs incubated with Tf as in state III. The corresponding time correlation function is shown in Figure 4b as state III*. Here, the $G(0)$ value is smaller than for 50% coated NPs, meaning a larger number of fluorescent objects. The experiment was repeated for PSCOOH NPs in the strong binding regime. Again, we find no change in the normalized number of NPs over time indicating that there is no exchange of proteins among NPs (Figure 4c).

We now aim to study the reversibility of proteins in the soft corona. To this end nanoparticles were fully covered with the equivalent of a full monolayer of unlabeled Tf (dark layer, Figure 5a). Subsequently fluorescently labeled Tf-488 was added forming a secondary layer with a fraction bound of approximately 0.4. In a third step unlabeled Tf was added and the exchange of labeled and unlabeled Tf monitored over time using the FCS signal. Figure 5b shows a decrease of the fraction bound of the protein (the slowly diffusing fraction) as a function of the added protein. The exchange between labeled and unlabeled protein occurs within a few seconds ($k_{off} \gg 1\ min^{-1}$).

Competitive Binding of Proteins to NPs. To address at least some elements of the effect of protein exchange in a complex biological fluid we chose to study Tf-NP in blood plasma. Again, NPs were incubated with the equivalent amount of a full monolayer of protein forming a hard corona. We then added plasma (5% and 10%) and followed the change of fraction bound over time. Figure 6 shows that no Tf-488 was removed by plasma. The hard corona appeared stable for hours. In contrast the soft corona showed exchange of protein. NPs with a fluorescently labeled soft corona were prepared as previously shown in Figure 5a using unlabeled Tf in the first monolayer, and coating the NPs with Tf-488 to the nominal fraction bound 0.6. Then, further addition of plasma proteins replaced Tf-488 in the secondary layers. We find off-rates $k_{off}(5\%) = 0.038\ min^{-1}$ and $k_{off}(10\%) = 0.08\ min^{-1}$ for 5% and 10% blood plasma concentration, respectively.

Interestingly, in the same kind of experiment, the off-rates of Transferrin from PSCOOH NPs are considerably faster. The soft corona of PSCOOH NPs has an off-rate of roughly $1\ min^{-1}$ in 5% plasma. Moreover, Tf proteins are totally removed from the PSCOOH NP surface already in 5% plasma, whereas a significant amount of Tf was still present on the $PSOSO_3H$ surfaces.

Furthermore we observed that the addition of 5% plasma to carboxylated (PSCOOH) NPs coated with only a monolayer of protein gave rise to aggregates, the size of which is too large to be measured properly with FCS.

CONCLUSION

We used FCS to measure the fraction bound of the blood protein, Transferrin, to sulfonate ($PSOSO_3H$) and carboxyl- (PSCOOH) polystyrene NPs. We measured the molar concentrations of fluorescently labeled proteins free in solution and bound to the NP surface. Hence, binding was studied in terms of number of molecules bound per particle. The adsorption curves show a universal behavior as a function of the molar protein to NP ratio indicating a clear transition from monolayer coverage to multilayer adsorption. Furthermore, this study reveals for the first time the existence of two time-scales in the dynamics of the protein adsorption layer. The two time scales fall in place with the proteins being bound in the first monolayer (hard corona) or being part of the secondary and ternary layers (soft corona). While the hard corona shows off-rate longer than the experimental time scale of a few hours, the soft corona appears to exchange proteins on the time scale faster than minutes under buffer conditions. We also note that the soft-corona time scale is increased in blood plasma, where Transferrin appears to come off within several minutes from $PSOSO_3H$ NPs depending on the concentration of blood plasma itself. Most importantly, however, we find the same split-up in the off-kinetics on PSCOOH NPs as on $PSOSO_3H$ NPs, albeit the off-kinetics of the soft corona in this case was considerably faster. In general, however, we find the distinction of hard and soft corona corroborated in terms of an irreversibly (or at least very long-lived) *versus* reversibly bound protein layer.

Extremely slow exchange rates or irreversible binding clearly is an issue that cannot be omitted when the effect of NPs on biological systems is studied. It implies that the order of protein exposure leaves behind a pattern of irreversibly bound proteins, which provides NPs with a unique fingerprint or "memory function", which will be hard to grasp. This notion has a primary impact on how the modeling of protein adsorption to nanoparticles surfaces should be approached. On the other hand the existence of a strongly bound monolayer might be practically helpful for research that aims at functionalization of nanoparticle-based drug carriers for biomedical use using protein adsorption.

EXPERIMENTAL SECTION

Materials. Polystyrene latex beads, sulfonated-modified $PSOSO_3H$ (nominally 100 nm), and carboxy-modified PSCOOH (nominally 100 and 50 nm), were purchased from Polysciences Inc. (Warrington, USA). Nanoparticles were characterized by measuring their size and *z*-potential in physiological buffer before use. Fluorescent Transferrin conjugates Alexa-488 were purchased by Invitrogen by Life Technology and dissolved to get 5 mg/mL stock solution in PBS (Sigma) and conserved as recommended from the supplier. Unlabeled holo-Transferrin (MW: 76−81 kDa) was provided from Sigma. Blood was withdrawn from 10 to 15 different volunteers and collected into 10 mL of K_2EDTA coated tubes (BD Bioscience) and stored at −80 °C until use. The plasma used in experiments, was allowed to thaw at room temperature and centrifuged for 3 min at 16.2kRCF.[47] All data presented are obtained using plasma from one donation session. The blood donation procedure was approved by the Human Research Ethics committee at University College Dublin.

Methods. *Fluorescence Correlation Spectroscopy.* FCS measurements were performed on an Axiovert 200 microscope with a ConfoCor 2 unit (Carl Zeiss, Jena, Germany). An argon ion laser (488 nm) was used for excitation. The objective was a 40× water immersion (Carl Zeiss Jena, Germany). Fluorescence emission was separated from the laser light using a bandpass filter 525/25. Measurements were performed at room temperature (22 °C) in a volume of at least 250 μL. Samples were measured in eight well LabTek II chamber slides (nunc, Wiesbaden, Germany). To minimize the absorption of proteins on the wall of the chamber a precoating was performed. Briefly, we added a low concentration of sonicated unilamellar vesicles formed from PC to the chambers and incubated them overnight. Before use, we rinsed the chambers gently with buffer to remove free sonicated unilamellar vesicles.

For the analysis of the fluorescence autocorrelation function we follow the procedure described in Rusu *et al.*[39] The measured autocorrelation functions were fitted using a two component function

$$G(\tau) = A_{\text{free}} g(\tau/\tau_{\text{free}}) + A_{\text{bound}} g(\tau/\tau_{\text{bound}}) = \frac{N_{\text{Tf\_free}} \cdot g(\tau/\tau_{\text{free}}) + N_{\text{NP}} \cdot q^2 \cdot g(\tau/\tau_{\text{bound}})}{(N_{\text{Tf\_free}} + N_{\text{NP}} \cdot q)^2} \quad (3)$$

with q meaning the ratio of the fluorescent yield of nanoparticles coated by proteins to that of free protein. It represents the average number of proteins bound per particle. In eq 3 τ_{free} and τ_{bound} are the correlation times for free and bound Transferrin, respectively, where each correlation function is given by

$$g(\tau/\tau_i) = \left(1 + \frac{T}{1-T} e^{-\tau/\tau_T}\right)\left(\frac{1}{1+\tau/\tau_i}\right)\left(\frac{1}{1+\tau/(S^2\tau_i)}\right)^{1/2} \quad (4)$$

Here T and τ_T represent the percentage of molecules in the triplet state and its relaxation time. S is the structural parameter (see also Supporting Information). The amplitudes A_{free} and A_{bound} are determined by the

number of Transferrin molecules per focal volume in solution, N_{Tf_free}, and the number of nanoparticles, N_{NP}, which are weighted by the number q of bound Transferrins.

The total number of Transferrin molecules in the focal volume is for the mass conservation $N_0 = N_{free} + N_{Tf\_bound}$, with N_{Tf_bound} number of proteins bound to the nanoparticles, in other words $N_{NP}q$. The analysis assumes that $q > 1$, that is, each NP is covered with at least one Transferrin and that no quenching of the chromophore has to be taken into account. In the Supporting Information it is shown that these assumptions hold and that measurements fall within the regime of reliable amplitude measurements. Using the expression for A_{free} from eq 3 and the mass conservation, we find $A_{free} = N_{free}/(N_0)^2$. Therefore, the fraction of bound Transferrins is determined by measuring the amplitude of Transferrin remaining free in solution and the total number of proteins:

$$f = \frac{N_{Tf\_bound}}{N_o} = 1 - A_{free}N_o \qquad (5)$$

N_0 is calculated from one-component fit to data when only Transferrin is present in solution. The parameters τ_{free} and τ_{bound} are also determined from Transferrin solution only and saturated NPs, respectively, and kept as fixed parameters in the fitting. For further details regarding calibration and fitting see Supporting Information.

Conflict of Interest: The authors declare no competing financial interest.

Acknowledgment. J.R. acknowledges an ESF travel grant "Epitope 4397". S.M. sincerely acknowledges financial support from DAAD. Part of this work was conducted under the framework of the INSPIRE programme, funded by the Irish Government's Programme for Research in Third Level Institutions, Cycle 4, National Development Plan 2007-2013 (AP). The SFI SRC BioNanoInteract (07 SRC B1155) also supported the research reported here (F.B.B., K.D.). Project BisNano (NMP4-SL-2010-263878) is gratefully acknowledged.

Supporting Information Available: Measurements of the molecular weights by FCS, measurements of the particles size by DLS, FCS measurements performed with labeled NPs and unlabeled Tf and adsorption isotherms equations. This material is available free of charge *via* the Internet at http://pubs.acs.org.

REFERENCES AND NOTES

1. Cedervall, T.; Lynch, I.; Lindman, S.; Berggard, T.; Thulin, E.; Nilsson, H.; Dawson, K. A.; Linse, S. Understanding the Nanoparticle-Protein Corona Using Methods to Quantify Exchange Rates and Affinities of Proteins for Nanoparticles. *Proc. Natl. Acad. Sci. U.S.A.* **2007**, *104*, 2050–2055.
2. Lundqvist, M.; Stigler, J.; Cedervall, T.; Berggråd, T.; Flanagan, M. B.; Lynch, I.; Elia, G.; Dawson, K. The Evolution of the Protein Corona around Nanoparticles: A Test Study. *ACS Nano* **2011**, *5*, 7503–7509.
3. Aggarwal, P.; Hall, J. B.; McLeland, C. B.; Dobrovolskaia, M. A.; McNeil, S. E. Nanoparticle Interaction with Plasma Proteins as It Relates to Particle Biodistribution, Biocompatibility and Therapeutic Efficacy. *Adv. Drug Delivery Rev.* **2009**, *61*, 428–437.
4. Maiorano, G.; Sabella, S.; Sorce, B.; Brunetti, V.; Malvindi, M. A.; Cingolani, R.; Pompa, P. P. Effects of Cell Culture Media on the Dynamic Formation of Protein, Nanoparticle Complexes and Influence on the Cellular Response. *ACS Nano* **2010**, *4*, 7481–7491.
5. Nel, A. E.; Madler, L.; Velegol, D.; Xia, T.; Hoek, E. M. V.; Somasundaran, P.; Klaessig, F.; Castranova, V.; Thompson, M. Understanding Biophysicochemical Interactions at the Nano-Bio Interface. *Nat. Mater.* **2009**, *8*, 543–557.
6. Choi, H. S.; Ashitate, Y.; Lee, J. H.; Kim, S. H.; Matsui, A.; Insin, N.; Bawendi, M. G.; Semmler-Behnke, M.; Frangioni, J. V.; Tsuda, A. Rapid Translocation of Nanoparticles from the Lung Airspaces to the Body. *Nat. Biotechnol.* **2010**, *28*, 1300–1303.
7. Minchin, R. Nanomedicine: Sizing Up Targets with Nanoparticles. *Nat. Nanotechnol.* **2008**, *3*, 12–13.
8. Lundqvist, M.; Stigler, J.; Elia, G.; Lynch, I.; Cedervall, T.; Dawson, K. A. Nanoparticle Size and Surface Properties Determine the Protein Corona with Possible Implications for Biological Impacts. *Proc. Natl. Acad. Sci. U.S.A.* **2008**, *105*, 14265–14270.
9. Klein, J. Probing the Interactions of Proteins and Nanoparticles. *Proc. Natl. Acad. Sci. U.S.A.* **2007**, *104*, 2029–2030.
10. Oberdörster, G. Safety Assessment for Nanotechnology and Nanomedicine: Concepts of Nanotoxicology. *J. Intern. Med.* **2010**, *267*, 89–105.
11. Baier, G.; Costa, C.; Zeller, A.; Baumann, D.; Sayer, C.; Araujo, P. H. H.; Mailänder, V.; Musyanovych, A.; Landfester, K. BSA Adsorption on Differently Charged Polystyrene Nanoparticles Using Isothermal Titration Calorimetry and the Influence on Cellular Uptake. *Macromol. Biosci.* **2011**, *11*, 628–638.
12. Lindman, S.; Lynch, I.; Thulin, E.; Nilsson, H.; Dawson, K. A.; Linse, S. Systematic Investigation of the Thermodynamics of HSA Adsorption to *N*-iso-propylacrylamide/*N*-tert-butylacrylamide Copolymer Nanoparticles. Effects of Particle Size and Hydrophobicity. *Nano Lett.* **2007**, *7*, 914–920.
13. Chakraborty, S.; Joshi, P.; Shanker, V.; Ansari, Z. A.; Singh, S. P.; Chakrabarti, P. Contrasting Effect of Gold Nanoparticles and Nanorods with Different Surface Modifications on the Structure and Activity of Bovine Serum Albumin. *Langmuir* **2011**, *27*, 7722–7731.
14. Bousquet, Y.; Swart, P. J.; Schmitt-Colin, N.; Velge-Roussel, F.; Kuipers, M. E.; Meijer, D. K. F.; Bru, N.; Hoebeke, J.; Breton, P. Molecular Mechanisms of the Adsorption of a Model Protein (Human Serum Albumin) on Poly(Methylidene Malonate 2.1.2) Nanoparticles. *Pharm. Res.* **1999**, *16*, 141–147.
15. Brewer, S. H.; Glomm, W. R.; Johnson, M. C.; Knag, M. K.; Franzen, S. Probing BSA Binding to Citrate-Coated Gold Nanoparticles and Surfaces. *Langmuir* **2005**, *21*, 9303–9307.
16. Walczyk, D.; Bombelli, F. B.; Monopoli, M. P.; Lynch, I.; Dawson, K. A. What the Cell "Sees" in Bionanoscience. *J. Am. Chem. Soc.* **2010**, *132*, 5761–5768.
17. Dusinska, M.; Dusinska, M.; Fjellsbø, L. M.; Magdolenova, Z.; Rinna, A.; Runden Pran, E.; Bartonova, A.; Heimstad, E. S.; Harju, M.; Tran, L.; *et al.* Testing Strategies for the Safety of Nanoparticles Used in Medical Applications. *Nanomedicine* **2009**, *4*, 605–607.
18. Deng, Z. J.; Mortimer, G.; Schiller, T.; Musumeci, A.; Martin, D.; Minchin, R. F. Differential Plasma Protein Binding to Metal Oxide Nanoparticles. *Nanotechnology* **2009**, *20*, 455101.
19. Fertsch-Gapp, S.; Semmler-Behnke, M.; Wenk, A.; Kreyling, G. W. Binding of Polystyrene and Carbon Black Nanoparticles to Blood Serum Proteins. *Inhalation Toxicol.* **2011**, *23*, 468–475.
20. Schulze, C.; Schaefer, U. F.; Ruge, C. A.; Wohlleben, W.; Lehr, C. M. Interaction of Metal Oxide Nanoparticles with Lung Surfactant Protein A. *Eur. J. Pharm. Biopharm.* **2011**, *77*, 376–383.
21. Lacerda, S. H. D. P.; Park, J. J.; Meuse, C.; Pristinski, D.; Becker, M. L.; Karim, A.; Douglas, J. F. Interaction of Gold Nanoparticles with Common Human Blood Proteins. *ACS Nano* **2009**, *4*, 365–379.
22. Tsai, D.-H.; Davila-Morris, M.; DelRio, F. W.; Guha, S.; Zachariah, M. R.; Hackley, V. A. Quantitative Determination of Competitive

Molecular Adsorption on Gold Nanoparticles Using Attenuated Total Reflectance, Fourier Transform Infrared Spectroscopy. *Langmuir* **2011**, *27*, 9302–9313.
23. Roach, P.; Farrar, D.; Perry, C. C. Surface Tailoring for Controlled Protein Adsorption: Effect of Topography at the Nanometer Scale and Chemistry. *J. Am. Chem. Soc.* **2006**, *128*, 3939–3945.
24. Leng, X. J.; Starchev, K.; Buffle, J. Adsorption of Fluorescent Dyes on Oxide Nanoparticles Studied by Fluorescence Correlation Spectroscopy. *Langmuir* **2002**, *18*, 7602–7608.
25. Jiang, X.; Weise, S.; Hafner, M.; Rocker, C.; Zhang, F.; Parak, W. J.; Nienhaus, G. U. Quantitative Analysis of the Protein Corona on FePt Nanoparticles Formed by Transferrin Binding. *J. R. Soc., Interface* **2010**, *7*, S5–S13.
26. Rocker, C.; Potzl, M.; Zhang, F.; Parak, W. J.; Nienhaus, G. U. A Quantitative Fluorescence Study of Protein Monolayer Formation on Colloidal Nanoparticles. *Nat. Nanotechnol.* **2009**, *4*, 577–580.
27. Shao, L. W.; Dong, C. Q.; Sang, F. M.; Qian, H. F.; Ren, J. C. Studies on Interaction of CdTe Quantum Dots with Bovine Serum Albumin Using Fluorescence Correlation Spectroscopy. *J. Fluoresc.* **2009**, *19*, 151–157.
28. Maffre, P.; Nienhaus, K.; Amin, F.; Parak, W. J.; Nienhaus, G. U. Characterization of Protein Adsorption onto FePt Nanoparticles Using Dual-Focus Fluorescence Correlation Spectroscopy. *Beilstein J. Nanotechnol.* **2011**, *2*, 374–383.
29. Norde, W.; Gonzalez, F. G.; Haynes, C. A. Protein Adsorption on Polystyrene Latex Particles. *Polym. Adv. Tech.* **1995**, *6*, 518–525.
30. Norde, W.; Lyklema, J. The Adsorption of Human Plasma Albumin and Bovine Pancreas Ribonuclease at Negatively Charged Polystyrene Surfaces: V. Microcalorimetry. *J. Colloid Interface Sci.* **1978**, *66*, 295–302.
31. Norde, W.; Lyklema, J. The Adsorption of Human Plasma Albumin and Bovine Pancreas Ribonuclease at Negatively Charged Polystyrene Surfaces: I. Adsorption Isotherms. Effects of Charge, Ionic Strength, and Temperature. *J. Colloid Interface Sci.* **1978**, *66*, 257–265.
32. Casals, E.; Pfaller, T.; Duschl, A.; Oostingh, G. J.; Puntes, V. Time Evolution of the Nanoparticle Protein Corona. *ACS Nano* **2010**, *4*, 3623–3632.
33. Monopoli, M. P.; Walczyk, D.; Campbell, A.; Elia, G.; Lynch, I.; Bombelli, F. B.; Dawson, K. A. Physical-Chemical Aspects of Protein Corona: Relevance to *in Vitro* and *in Vivo* Biological Impacts of Nanoparticles. *J. Am. Chem. Soc.* **2011**, *133*, 2525–2534.
34. Vroman, L.; Adams, A. L. Identification of Rapid Changes at Plasma-Solid Interfaces. *J. Biomed. Mater. Res.* **1969**, *3*, 43–67.
35. Cedervall, T.; Lynch, I.; Foy, M.; Berggard, T.; Donnelly, S. C.; Cagney, G.; Linse, S.; Dawson, K. A. Detailed Identification of Plasma Proteins Adsorbed on Copolymer Nanoparticles. *Angew. Chem., Int. Ed. Engl.* **2007**, *46*, 5754–5756.
36. Monopoli, M. P.; Bombelli, F. B.; Dawson, K. A. Nanobiotechnology: Nanoparticle Coronas Take Shape. *Nat. Nanotechnol.* **2011**, *6*, 11–12.
37. Kreyling, W. G.; Hirn, S.; Schleh, C. Nanoparticles in the Lung. *Nat. Biotechnol.* **2010**, *28*, 1275–1276.
38. Wohlfart, S.; Gelperina, S.; Kreuter, J., Transport of Drugs Across the Blood, Brain Barrier by Nanoparticles. *J. Controlled Release*.
39. Rusu, L.; Gambhir, A.; McLaughlin, S.; Rädler, J. Fluorescence Correlation Spectroscopy Studies of Peptide and Protein Binding to Phospholipid Vesicles. *Biophys. J.* **2004**, *87*, 1044–1053.
40. Engelke, H.; Lippok, S.; Dorn, I.; Netz, R.; Rädler, J. FVIII Binding to PS Membranes Differs in the Activated and Non-activated Form and Can Be Shielded by Annexin A5. *J. Phys. Chem. B.* **2011**, *115*, 12963–12970.
41. Engelke, H.; Dorn, I.; Rädler, J. O. Diffusion and Molecular Binding in Crowded Vesicle Solutions Measured by Fluorescence Correlation Spectroscopy. *Soft Matter* **2009**, *5*, 4283–4289.
42. Pack, D. W.; Hoffman, A. S.; Pun, S.; Stayton, P. S. Design and Development of Polymers for Gene Delivery. *Nat. Rev. Drug Discovery* **2005**, *4*, 581–593.
43. Armstrong, J. K.; Wenby, R. B.; Meiselman, H. J.; Fisher, T. C. The Hydrodynamic Radii of Macromolecules and Their Effect on Red Blood Cell Aggregation. *Biophys. J.* **2004**, *87*, 4259–4270.
44. Bailey, S.; Evans, R. W.; Garratt, R. C.; Gorinsky, B.; Hasnain, S.; Horsburgh, C.; Jhoti, H.; Lindley, P. F.; Mydin, A. Molecular Structure of Serum Transferrin at 3.3-Å Resolution. *Biochemistry* **1988**, *27*, 5804–5812.
45. Verrecchia, T.; Huve, P.; Bazile, D.; Veillard, M.; Spenlehauer, G.; Couvreur, P. Adsorption/Desorption of Human Serum Albumin at the Surface of Poly(lactic acid) Nanoparticles Prepared by a Solvent Evaporation Process. *J. Biomed. Mater. Res.* **1993**, *27*, 1019–1028.
46. Kowalczynska, H. M.; Nowak-Wyrzykowska, M.; Szczepankiewicz, A. A.; Dobkowski, J.; Dyda, M.; Kaminski, J.; Kolos, R. Albumin Adsorption on Unmodified and Sulfonated Polystyrene Surfaces, in Relation to Cell-Substratum Adhesion. *Colloids Surf., B* **2011**, *84*, 536–544.
47. Rai, A. J.; Gelfand, C. A.; Haywood, B. C.; Warunek, D. J.; Yi, J.; Schuchard, M. D.; Mehigh, R. J.; Cockrill, S. L.; Scott, G. B. I.; Tammen, H.; *et al*. HUPO Plasma Proteome Project Specimen Collection and Handling: Towards the Standardization of Parameters for Plasma Proteome Samples. *Proteomics* **2005**, *5*, 3262–3277.